https://doi.org/10.46813/2023-145-026

STRUCTURE OF MASS DISTRIBUTIONS OF PHOTOFISSION PRODUCT YIELDS OF ^{238}U AT 17.5 MeV BREMSSTRAHLUNG ENERGY

E.V. Oleynikov, O.O. Parlag, I.V. Pylypchynets, V.T. Maslyuk, O.I. Lengyel*
Institute of Electron Physics, NAS of Ukraine, Uzhhorod, Ukraine
**E-mail: parlag.oleg@gmail.com*

The values of 29 relative yields of products belonging to 26 mass chains of photofission of ^{238}U were obtained at a maximum bremsstrahlung energy of 17.5 MeV (near the second chance fission threshold). The stimulation of the ^{238}U photofission reaction was performed at the electron accelerator of the Institute of Electron Physics of the National Academy of Sciences of Ukraine, the M-30 microtron. The GEANT4 toolkit was used to model the components of the bremsstrahlung spectrum. The presence of a fine structure in the mass distribution of heavy product yields was found to be localized in the mass range 133-134, 138-139, and 143-144. A multi gaussian model (superposition of three Gaussians) was used to theoretically describe the structure. The calculated values of product yields using the GEF code describe in general terms and predict the fine structure of the mass distribution of photofission products of ^{238}U.

PACS: 24.75.+1, 25.85.-w, 25.85.Ec, 25.85. Ca

INTRODUCTION

Product (fragment) yields are one of the main parameters characterizing the fission process of actinide nuclei. The values of mass distributions of product yields are a source of information on the influence of the nuclear structure on the fission process [1]. Existing experimental data on the yields of fission products (initiated by photons, neutrons, protons) for a wide range of actinide nuclei indicate the presence of a fine structure in their two–hump mass distributions [2, 3]. This structure is manifested in the increased yields of heavy fission products localized in the vicinity of masses 133-134, 138-140, and 143-144 and their complementary light products [3] and is associated with such effects of nuclear structure as the effect of proximity to closed nuclear shells and the odd-even effect [2, 4, 5].

One of the promising areas of researching the fission process is the study of mass distributions of fission products under the influence of photons since the nature of this interaction is well known [6] and allows for the production of fissile nuclei immediately after their absorption.

Of particular interest in terms of experimental and theoretical research is information on the yields of nucleus photon fission products of ^{238}U due to their use in solving a wide range of applied problems. These tasks are related to the development of new generation energy generating systems – reactors with accelerators (controlled subcritical systems [7]), methods for producing beams of neutron-overloaded exotic nuclei [8], non-destructive methods of isotopic analysis of fertile nuclear materials [9], alternative methods for the production of medical radioisotopes [10]. The above-mentioned areas require reliable data on the yields of photofission products of ^{238}U for a wide energy range.

Experimental studies of the yields of the photon fission products of the nucleus ^{238}U were carried out for the energy range of the giant dipole resonance (bremsstrahlung energy $E_{\gamma max}$ from 6.1 to 30.0 MeV, which corresponds to the excitation energy E^* of the fissile nucleus ^{238}U* – 5.6…14.7 MeV) [11], where the probabilities of reactions of both emission-free (^{238}U(γ,f)^{238}U* – first chance fission) and fission with preliminary emission of one neutron (^{238}U(γ,nf)^{237}U* - second chance (threshold energy ~ 12.6 MeV [12]), ^{238}U(γ,2nf)^{236}U* – third chance, and so on). That is, the fission process occurs after neutron evaporation, when the fissile nucleus with fewer neutrons will have a lower excitation energy, which demonstrates stronger shell effects than in the original constituent nucleus [13]. This explains the presence of a structure of mass distributions of photon fission products even at energies above the thresholds of fission with preliminary emission of particles. Therefore, it is of interest to conduct experimental studies for the energy region in the vicinity of the second-chance fission reaction threshold.

The existing experimental data on product yields at energies close to the second chance threshold of photofission of ^{238}U [3, 9, 14] describe only the shape of the mass distribution and do not allow us to draw an unambiguous conclusion about its structure due to the lack of a sufficient number of experimental points (at fixed fragment masses).

The aim of the present work is to study the experimental structure of the mass distribution of the outputs of the photon fission products of the ^{238}U nucleus at the maximum energy of 17.5 MeV, to analyze the data obtained within the framework of the multi gaussian (multimodal) fission model and the GEF code.

1. MATERIALS AND METHODS

The yields of photofission products of ^{238}U were determined by semiconductor gamma-ray spectrometry [15]. The experimentally investigated quantities in the measurements by this method are the count rate in γ-quantum peaks $n_i(E_\gamma)$ from individual fission products at fixed energies E_γ. Their values depend on the activity of the product, the absolute efficiency of measurements, the intensity of γ-lines, corrections for self-absorption, and are determined by formula (1) [15]:

$$n_i(E_\gamma) = q_i \varepsilon_i(E_\gamma) I_i(E_\gamma) s_i(E_\gamma), \quad (1)$$

where q_i is the activity (depends on the number of fission events in the sample), $\varepsilon_i(E_\gamma)$ is the spectrometer

efficiency for energy E_γ; $I_i(E_\gamma)$ is the absolute yield of the gamma line with energy E_γ; $s_i(E_\gamma)$ is the correction for self-absorption in the fragment collector for a given energy E_γ.

1.1. STIMULATION OF THE ^{238}U PHOTOFISSION REACTION ON THE M-30 MICROTRON

In the experimental studies, a rectangular plate of natural metal of ^{238}U was used (side dimensions of – 11 and 18 mm, thickness – 0.4 mm). For the accumulation of photofission products during the activation process, an aluminium (Al) foil with a thickness of 0.1 mm (its area was identical to the sample area) was used and installed close to the fission target of ^{238}U.

The fission assembly was irradiated using an electron accelerator of the IEP of NAS of Ukraine – the microtron M-30. The electron energy was 17.5 MeV, the average beam current was ~ 4 μA. The instability of electron energy during the irradiation of the target did not exceed 0.04 MeV [16]. The activation scheme of the sample is shown in Fig. 1.

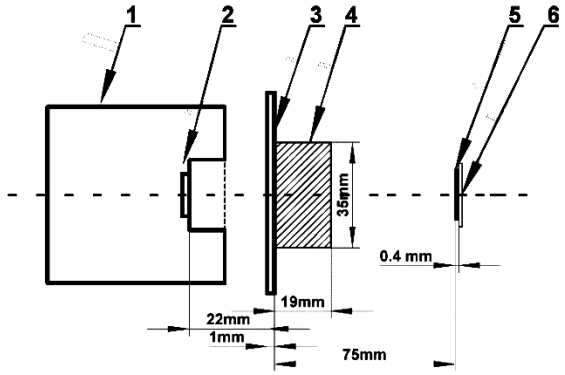

Fig. 1. Activation scheme of the ^{238}U sample on the M-30 microtron:
1 – electron output unit; 2 – window of the output unit (ellipse, thickness – 50 μm); 3 – electron-to-photon converter (Ta, 100x50x1 mm); 4 – filter B_4C (diameter – 30 mm, thickness – 19 mm); 5 – sample of ^{238}U; 6 – storage of photofission products (material – Al, thickness – 0.1 mm)

To generate bremsstrahlung, a tantalum (Ta) converter (thickness – 1 mm) was used, located at a distance of 22 mm from the output window (material – titanium (Ti), thickness – 50 μm) of the electron ejection unit. The filter for residual electrons and photoneutrons (B_4C) was installed close to the Ta converter perpendicular to the beam axis [17]. The splitter assembly (^{238}U + Al) was installed perpendicular to the beam axis at a distance of 75 mm from the Ta converter.

The irradiation time of the fission assembly varied from 5 to 10 min for individual experimental series. The choice of time parameters (irradiation, cooling, and measurement times) was made taking into account the half-lives of photon fission products and their precursors in the isobaric chain (the so-called "parent" products).

1.2. SIMULATION OF THE SAMPLE ACTIVATION PROCESS ^{238}U

The GEANT4 10.7 toolkit [18] was used to model the bremsstrahlung spectra, residual electrons, and secondary photoneutrons (normalized per electron) interacting with the sample under study. The input parameters used in the calculations almost completely reproduced the activation scheme of the sample and the design features of the electron output unit of the M-30 microtron [16].

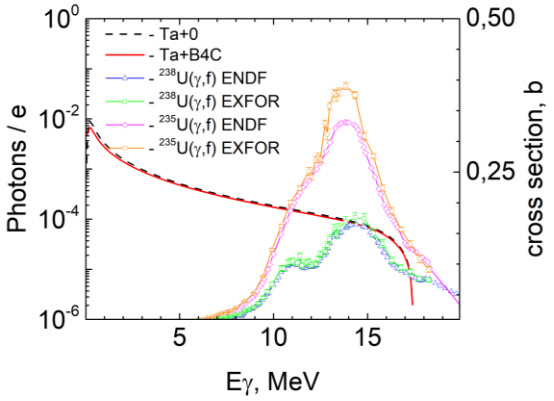

Fig. 2. Photon spectra (without and with B_4C filter) and cross sections of photofission reactions of ^{235}U and ^{238}U isotopes

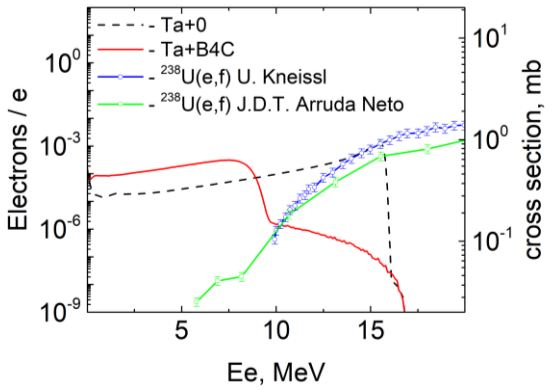

Fig. 3. Spectra of residual electrons (without and with B_4C filter) and cross sections of the electro-fission reaction of the ^{238}U isotope

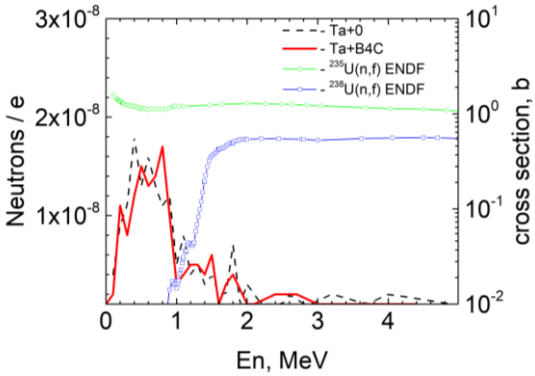

Fig. 4. Spectra of secondary photoneutrons (without and with B_4C filter) and cross sections of neutron fission reactions of ^{235}U and ^{238}U isotopes

The calculations were performed on a computer with a 6-core Intel(R)Core(TM)i7-9750HCPU@2.60 GHz and 32 GB of RAM for 10E+9 electrons in the initial beam.

The results of calculations of the bremsstrahlung spectra, residual electrons, and secondary photoneutrons falling on a sample of ^{238}U with and without a filter made of B_4C are shown in Figs. 2–4, respectively. The same figures show cross sections of the reactions of photo- [12, 19], electro- [20, 21], and neutron [19] fission of ^{235}U and ^{238}U nuclei.

The integral values of the fluxes of photons, residual electrons, and secondary photoneutrons normalized per electron falling on a sample of ^{238}U are 0.1136 photons (with energy > 6 MeV – 0.0172), 0.0157 electrons (with energy > 6 MeV – 0.0078), and 1.51E-7 photoneutrons.

The effect of the filter from the B_4C activation scheme on the final shape of the spectra of photons and residual electrons falling on the uranium sample is investigated.

The filter with B_4C absorbs photons – 10.8% (with energy > 6 MeV – 6.0%) of the total number of photons that hit the sample for the used experimental scheme, similarly, secondary electrons – 41.2% (with energy > 6 MeV – 69.2%), and secondary photoneutrons – 9.6%.

For the proposed scheme of stimulation of the photon fission reaction, 9.72% of photons and 2.81% of electrons of the total amount (those that fall into the plane of the sample – 1000x1000 mm) hit the uranium sample. Similarly, 12.51% of photons and 3.02% of electrons interact with the sample (energy > 6 MeV), respectively. Fig. 5 shows the profile of the photon beam in the plane (1000x1000 mm) of the sample location of ^{238}U, perpendicular to the axis of the initial electron beam and the sample under study.

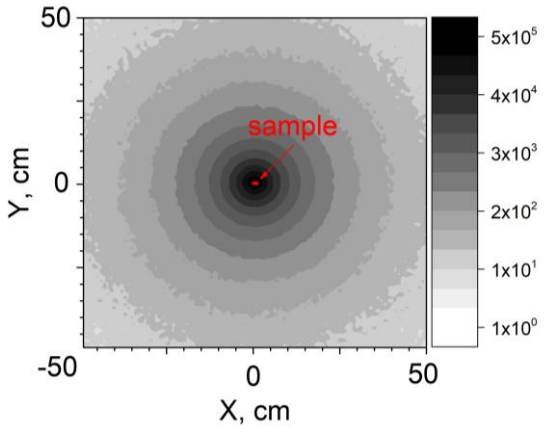

Fig. 5. Profile of the photon beam falling into the plane (1000 x 1000 mm) of the sample setup of ^{238}U perpendicular to the axis of the initial electron beam

The obtained values of photon fluxes, residual electrons, and photoneutrons were used to estimate the contribution of the yields of concomitant nuclear reactions via the channels ^{238}U(e,f), ^{235}U(γ,f), ^{235}U(n,f), and ^{238}U(n,f) to the yield of the photon fission reaction of ^{238}U during the irradiation time of 0…4 h according to (2).

$$Y(t) = Nt \int_{E_t}^{E_{max}} \varphi(E, E_{max})\sigma(E)dE, \qquad (2)$$

where $Y(t)$ is the number of uranium nuclear fission events; N is the number of uranium nuclei (^{238}U, ^{235}U) in the sample under study; t is the irradiation time of the sample; $\varphi(E, E_{max})$ – is the density of particle fluxes (photons, residual electrons, secondary photon neutrons) formed during irradiation of the converter with energy E; $\sigma(E)$ – values of the cross sections of reactions (photo-, electro-, neutron) of fission with energy E; E_{th} – threshold energy of reactions; E_{max} – maximum energy of reactions.

The calculations were based on the cross sections of (γ,f) and (n,f) reactions from the ENDF database [19], and experimental cross sections for the reactions ^{238}U(e,f) [20, 21], ^{235}U(γ,f) and ^{238}U(γ,f) [19] (data values from the EXFOR database tables [3]). The calculations took into account the percentage of isotopes in the uranium target: ^{238}U – 99.2742%, ^{235}U – 0.7204%.

The cross sections for photo-, electro-, and neutron fission are shown in Figs. 2–4, respectively. Fig. 6 shows the calculated curves of the dependence of reaction yields on activation time when the target of ^{238}U is irradiated with photons, residual electrons, and secondary photoneutrons.

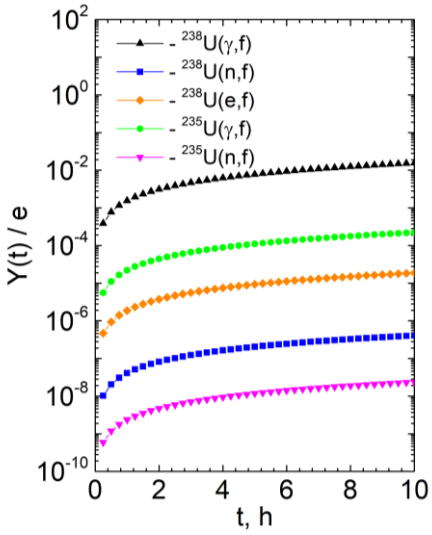

Fig. 6. Dependence of reaction yields on activation time (0…4 h) under bremsstrahlung irradiation of ^{238}U with energy of 17.5 MeV

The calculation results indicate that the yields of the products of the listed concomitant nuclear reactions do not significantly contribute to the yields of ^{238}U photofission products for the activation scheme used. Thus, during the interaction of photons, residual electrons, and secondary photoneutrons with the ^{238}U sample, the contribution of the considered reactions in percentage terms is: ~ 98.482% – ^{238}U(γ,f), ~ 1.397% – ^{235}U(γ,f), ~ 1.2E-1% – ^{238}U(e,f), ~ 1.49E-4% – ^{235}U(n,f), and 2.59E-3% – ^{238}U(n,f).

1.3. EXCITATION ENERGY OF THE FISSILE NUCLEUS ^{238}U AND THRESHOLDS OF MULTICHANCE PHOTOFISSION

For the fissile nucleus^{238} U, the excitation energy E* was calculated using formula (3) [22]:

$$E^* = \frac{\sum_{i=1}^{n} E_i \sigma(E_i, E_{\gamma\ max}) \Delta E \sigma_f(E_i)}{\sum_{i=1}^{n} \sigma(E_i, E_{\gamma\ max}) \Delta E \sigma_f(E_i)}, \qquad (3)$$

where $\sigma(E_i, E_{\gamma\ max})$ is the number of formed gamma quanta with energy E_i produced by an electron, $\sigma_f(E_i)$ is the value of the cross section of the photon fission reaction of the ^{238}U nucleus depending on the energy E_i [19] The bremsstrahlung spectrum $\sigma(E_i, E_{\gamma\ max})$ was calculated by a program created using the GEANT4 10.7 code libraries. The value of the excitation energy is 11.43 MeV.

To estimate the boundaries of the energy of emission-free region and photofission with preliminary neutron emission, we calculated the contribution of the partial cross sections of (γ,f)-, (γ,nf)-, (γ,2nf)-reactions to the full cross section of photofission (γ,F) and their thresholds using the Talys 1.96 code [23] (Fig. 7). The reaction thresholds are ~4.3 MeV (2.1E-3), ~10.8 MeV (12.07), and ~15.5 MeV (6.15E-3) for (γ,f)-, (γ,nf)-, and (γ,2nf)-reactions, respectively (cross sections at the indicated energies in millibars are given in parentheses). The obtained value of the total reaction cross section (γ,F) is consistent with the cross section value from the TENDL 2021 library (version 11 – TENDL-2021, which is based on both calculations and adjusted Talys calculations) [24].

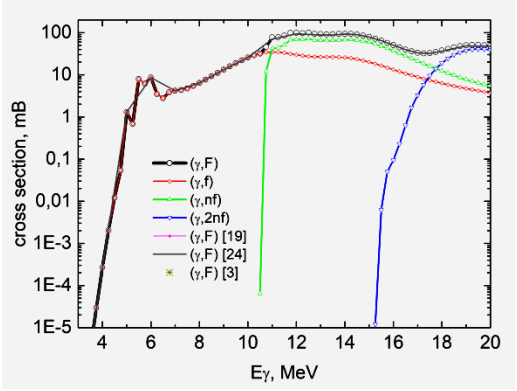

Fig. 7. Dependence of the total and partial cross sections of the photofission of ^{238}U on the photon energy

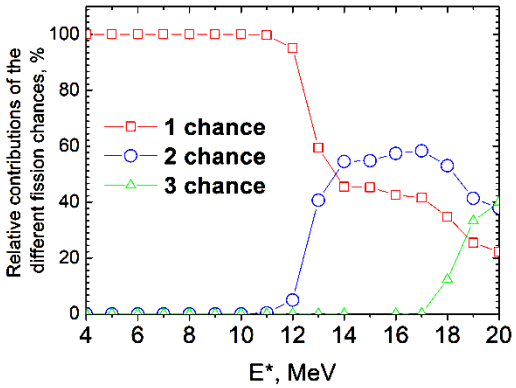

Fig. 8. Dependence of the relative contribution of individual fission probabilities on the excitation energy for the ^{238}U nucleus*

Additionally, we calculated the dependence of the probability of the relative contribution of individual fission chances to the total yield of products for the fissile nucleus of ^{238}U* on the excitation energy using the GEF code [25]. The results of the calculations are shown in Fig. 8. The relative contribution of the second chance does not exceed ~ 2% (0.019) at E* = 11.43 MeV.

1.4. SPECTROMETRY OF GAMMA RADIATION FROM PHOTOFISSION PRODUCTS OF ^{238}U

Spectrometric complexes based on semiconductor detectors were used to measure γ-radiation from the photofission products of ^{238}U: HPGe (ORTEC) and Ge(Li), whose volumes were 150 and 100 cm^3 with an energy resolution of ~ 2.45 and ~ 3.5 keV (for the line ^{60}Co – 1332.5 keV) [26,27]. Standard certified point sources of γ-radiation (^{22}Na, ^{57}Co, ^{60}Co, ^{109}Cd, ^{133}Ba, ^{137}Cs, ^{151}Eu, ^{241}Am) were used to determine the peak efficiency of the detectors. Additionally, the detectors were self-calibrated using γ-radiation from the photon fission products of ^{238}U accumulated in aluminium foil [28]. This made it possible to significantly simplify the measurement process and take into account the real geometry. The statistical error of the measurements during the calibration procedure did not exceed 4 %.

After the end of the accumulation of fragments by aluminium collectors, measurements of their gamma activity were performed within 0.2 to 491.3 h after the end of irradiation. The duration of individual series of measurements varied from 0.03 to 7.0 h.

Measurements of gamma spectra from photon fission products were performed in the live mode. The dead time of the spectrometer did not exceed 8%. During the measurements, the drift of the energy scale, resolution, and registration efficiency of the spectrometer complex was monitored using point standard gamma-active sources of ^{57}Co and ^{60}Co. The drift of these parameters did not exceed 1%.

The identification of the photofission products of ^{238}U was carried out by the energies of their characteristic gamma lines, taking into account their half-lives and the times of measurement, accumulation, and cooling. Additionally, the half-lives of their isobaric precursors were taken into account. The analysis was based on nuclear spectroscopic data from the NNDC library (USA) [29].

During the experiment, the peak intensity of the γ-lines of the following photofission products of the ^{238}U nucleus: ^{85m}Kr (151.2), ^{87}Kr (402.6), ^{88}Rb (1836.0), ^{89}Rb (1031.9), ^{91}Sr (749.8; 1024.3), ^{92}Sr (1383.9), ^{93}Y (266.9), ^{95}Zr (756.7), ^{97}Nb (657.94), ^{97}Zr (743.4), ^{99}Mo (739.5), ^{103}Ru (497.1), ^{105}Ru (724.21), ^{129}Sb (812.9), ^{131}I (364.5), ^{132}Te (228.2), ^{133}I (529.9), ^{134}Te (767.2), ^{134}I (847.0; 884.1), ^{135}I (1260.4), ^{138}Xe (434.6), ^{138}Cs (1009.8), ^{139}Ba (165.9), ^{140}La (815.8), ^{141}Ce (145.4), ^{142}La (641.3), ^{143}Ce (293.3), ^{147}Nd (91.1), ^{149}Nd (211.3). Energy E_γ (in keV) is given in parentheses.

The statistical error of the measurements of the intensity of the γ-lines of the photofission of ^{238}U products did not exceed 3…5% for the entire time interval of measurements.

The spectroscopic information was processed using the Winspectrum software package [30].

RESULTS AND DISCUSSION

As a result of the experimental studies, the relative yields of 29 products ^{85m}Kr, ^{87}Kr, ^{88}Rb, ^{89}Rb, ^{91}Sr, ^{92}Sr, ^{93}Y, ^{95}Zr, ^{97}Nb, ^{97}Zr, ^{99}Mo, ^{103}Ru, ^{105}Ru, ^{129}Sb, ^{131}I, ^{132}Te, ^{133}I, ^{134}Te, ^{134}I, ^{135}I, ^{138}Xe, ^{138}Cs, ^{139}Ba, ^{140}La, ^{141}Ce, ^{142}La, ^{143}Ce, ^{147}Nd, ^{149}Nd, which belong to 26 mass chains. The yields of photofission products were

determined relative to the yield of ^{132}Te [9], which was used as a reference point.

The total error of the product yields was estimated taking into account the statistical errors of their γ-lines intensities, analysis of time dependencies (irradiation, cooling, and measurements), scatter of values averaged over individual series of measurements, errors of interpolated efficiency values and nuclear spectrometric constants (energy and intensity of γ-lines, half-lives of products and their precursors in the isobaric chain). The total error in determining the relative yields of fission products did not exceed 10%.

The values of the relative and normalized yields of the products of ^{238}U photofission are shown in Fig. 9 by black and light circles, respectively. The rhombuses, upper triangles, squares, and lower triangles represent the product yields at maximum braking radiation energies of 16.3 [14], 17.2 [11], and 17.5 [9] and 19.4 MeV [14]. The presented experimental data are consistent with each other within the experimental errors for most experimental points.

The obtained mass distribution of photofission yields of ^{238}U products shows a structure (for heavy fragments with mass numbers 134, 138, and 143, the yield is increased).

Higher yields of photon fission products localized in the vicinity of the mentioned mass numbers (A) 133-134, 138-139, and 143-144, and complementary light mass fission products, are associated with the effect of nuclear structure, such as the influence of nuclear shells on the fragment formation process and the odd-even effect [2, 4, 5, 11].

According to the multimodal model of Brosa [4, 5], higher yields of products localized in the vicinity of masses 133-135 and 143-145 and complementary light products are explained by asymmetric fission channels (modes) – Standard I and Standard II, which are associated with the influence of shells. Higher yields of products with masses 133-134 are due to the presence of a spherical neutron shell – 82n. The number of neutrons n = 82 is assumption of one neutron emission for A=133-134 with the most probable charge Z = 52 [2, 11]. Similarly, the higher yields of products with masses 143-144 are due to the presence of a deformed neutron shell – 88n. The number of neutrons n = 88 is assumption of two neutron emission for A = 143-144 with Z = 56. For mass numbers 133-134, 138-140, and 143-144, the highest yields of heavy and complementary light products are in the range of five mass and two charge units [2, 11]. The values of the most probable charges corresponding to the masses A = 133-134, 138-140, and 143-144 are even Z = 52, 54, and 56. Thus, the difference of two even charges leads to higher yields for these products in the range of five mass units [2, 11].

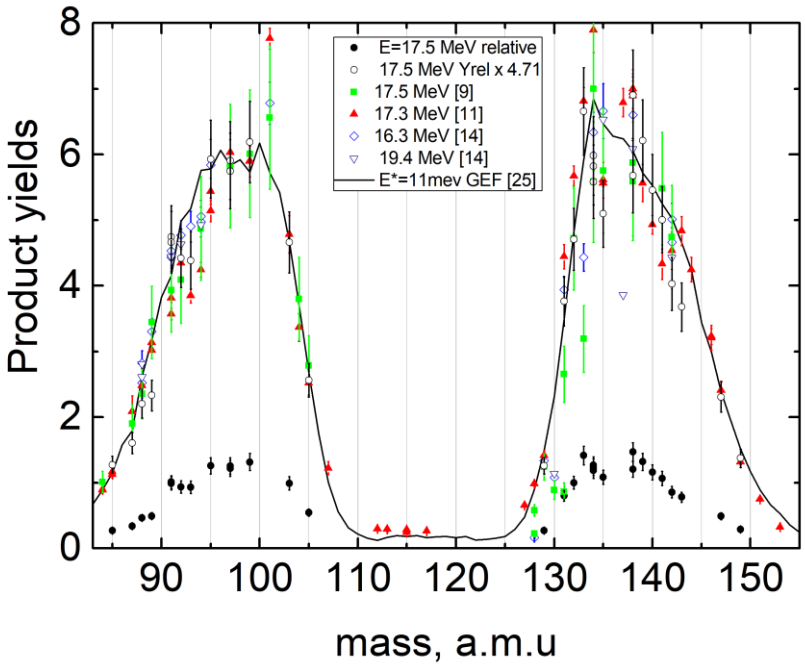

Fig. 9. ^{238}U photofission products yields

Additionally, Fig. 9 shows the fission product yields for the fissile nucleus ^{238}U* at an excitation energy of ~ 11.43 MeV calculated by the GEF code [24] (solid curve), which generally describes the dependence of product yields on the mass of fragments and predicts its structure.

To study (analyze) the structure of the mass distribution of heavy photofission products of ^{238}U, we described it by the superposition of three Gaussians [31]. For the description, formula (4) was used:

$$Y_i(A) = \sum_{i=1}^{3} \frac{W_i}{\sqrt{2\pi\sigma_{A,i}}} exp\left(-\frac{(A-A_{H,i})^2}{2\sigma_{Ai}^2}\right), \qquad (4)$$

where $A_{H,i}$ are the most probable masses of heavy fragments; σ_{Ai} are the variances of the mass distributions of fragments; W_i are the probabilities of the outputs of individual fission channels (or Gaussian areas) with centers localized in the vicinity of the most probable masses of heavy fragments (~134, ~138, and ~143).

To approximate the mass distribution of the experimental data on the yields of heavy products by a

superposition of three Gaussians, the CERN MINUIT least-squares program was used [32]. In addition to the data obtained, the available experimental data at close excitation energies were used for analysis (see Fig. 9).

The most adequate description was obtained with fixed values of the peak positions and variance of the Gaussians: A1 = 133.5, σ1 = 1.35; A2 =138, σ2 = 1.5 s; A3 = 143, σ3 = 4 a.m.u.

The results of our calculations (Fig. 10) confirm the presence of 3 peaks of fine structure (4) in the mass distribution of the photofission of ^{238}U.

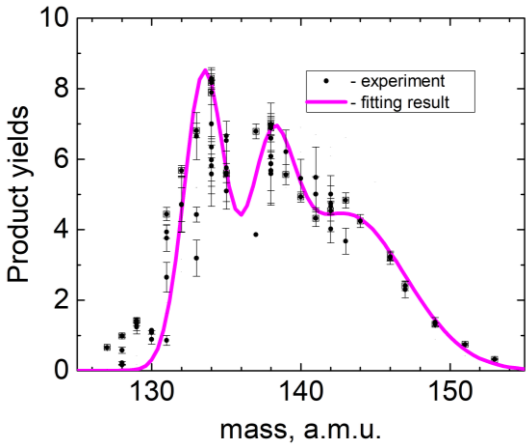

Fig. 10. Description of the experimental values of the photofission yields of heavy products of ^{238}U by a superposition of three Gaussians

CONCLUSIONS

The relative yields of 29 (for 26 mass chains) photofission products of ^{238}U at the maximum bremsstrahlung energy of 17.5 MeV in the vicinity of the second chance fission threshold have been determined by semiconductor γ-spectroscopy.

The results of modelling the characteristics of the bremsstrahlung beam and its components (the ratio of photons, residual electrons, and secondary photoneutrons) falling on the sample under study allowed us to develop an optimal scheme for stimulating the photofission reaction of actinide nuclei on the M-30 microtron, which ensures that products from concomitant nuclear reactions do not contribute to the yields of photofission products.

The description of the data obtained together with the use of available experimental data at close excitation energies within the bounds of the multi gaussian model indicates the stable presence of a fine structure of the mass distributions of the heavy products of ^{238}U photofission localized in the vicinity of masses 133-134, 138-139, and 143-144. The model calculations performed by the GEF code describe and predict the structure of mass distributions for the fissile nucleus ^{238}U at an average excitation energy of 11.43 MeV.

ACKNOWLEDGEMENTS

The authors express their gratitude to the microtron group (Y. Gainish, G. Pitchenko, O. Turkhovsky) for the uninterrupted operation of the accelerator and to I. Kushtan for the technical support of the experimental studies.

REFERENCES

1. K.-H. Schmidt, B. Jurado. Review on the progress in nuclear fission – experimental methods and theoretical descriptions // *Rep. Prog. Phys.* 2018, v. 81, 106301. https://doi.org/10.1088/1361-6633/aacfa7
2. H. Naik, G.N. Kim, S.V. Suryanarayana, et al. Studies on Neutron, Photon (Bremsstrahlung) and Proton Induced Fission of Actinides and Pre-Actinides // *J. Nucl. Phy. Mat. Sci. Rad. A.* 2015, v. 3, p. 55-73. https://doi.org/10.15415/jnp.2015.31008
3. Experimental Nuclear Reaction Data (EXFOR). Database Version of 2023-01-20. https://www-nds.iaea.org/exfor/
4. U. Brosa, S. Grossmann. A. Muller Nuclear scission // *Phys. Report.* 1990, v. 197, p. 167-262. https://doi.org/10.1016/0370-1573(90)90114-H
5. S. Oberstedt, F.-J. Hambsch, F. Vivès. Fission-mode calculations for ^{239}U, a revision of the multi-modal random neck-rupture model // *Nucl. Phys. A.* 1998, v. 644, p. 289-305. https://doi.org/10.1016/S0375-9474(98)00598-3
6. A. Zilges, D.L. Balabanski, J. Isaak, N. Pietrall. Photonuclear reactions – From basic research to applications // *Progress in Particle and Nuclear Physics.* 2022, v. 122, p. 103903. https://doi.org/10.1016/j.ppnp.2021.103903
7. S. Stoulos, M. Fragopoulou, E. Vagena, et al. Electron accelerator driven system for transmutation studies // *J. Rad. Nucl. Chem.* 2018, v. 318, p. 1209-1217. https://doi.org/10.1007/s10967-018-6218-1
8. B. Mei, D.L. Balabanski, P. Constantin, et al. Empirical parametrization for production cross sections of neutron-rich nuclei by photofission of ^{238}U at low energies // *Phys. Rev. C.* 2017, v. 96, p. 064610. https://doi.org/10.1103/PhysRevC.96.064610
9. M. Delarue, E. Simon, B. Perot, et al. New measurements of cumulative photofission yields of ^{239}Pu, ^{235}U and ^{238}U with a 17.5 MeV Bremsstrahlung photon beam and progress toward actinide differentiation // *Nucl. Inst. Meth. A.* 2022, v. 1040, p. 167259. https://doi.org/10.1016/j.nima.2022.167259
10. H. Naik, S.V. Suryanarayana, K.C. Jagadeesan, et al. An alternative route for the preparation of the medical isotope ^{99}Mo from the ^{238}U(γ,f) and ^{100}Mo(γ,n) reactions // *J Rad Nucl Chem.* 2013, v. 295, p. 807-816. https://doi.org/10.1007/s10967-012-1958-9
11. H. Naik, F. Carrel, G.N. Kim, et al. Mass yield distributions of fission products from photofission of ^{238}U induced by 11.5…17.3 MeV bremsstrahlung // *Eur. Phys. J. A.* 2013, v. 49, p. 94. https://doi.org/10.1140/epja/i2013-13094-7
12. J.T. Caldwell, E.J. Dowdy, B.L. Berman, et al. Giant resonance for the actinide nuclei: Photoneutron and photofission cross sections for ^{235}U, ^{236}U, ^{238}U, and ^{232}Th // *Phys. Rev. C.* 1980, v. 21, p. 1215-1231. https://doi.org/10.1103/PhysRevC.21.1215

13. S. Tanaka, K. Hirose, K. Nishio, Y. Aritomo. Role of multi-chance fission in highly excited heavy nuclei // *JPS Conf. Proc.* 2020, v. 32, 010004. https://doi.org/10.7566/JPSCP.32.010004
14. F. Carrel, M. Agelou, M. Gmar, et al. New experimental results on the cumulative yields from thermal fission of ^{235}U and ^{239}Pu and from photofission of ^{235}U and ^{238}U induced by bremsstrahlung // *IEEE Trans. Nucl. Sci*. 2011, v. 58, p. 2064-2072. https://doi.org/10.1109/TNS.2011.2157169
15. N.I. Zaika, Y.V. Kibkalo, A.I. Lendel, et al. Determination of angular distributions of fission fragments from isolated masses by semiconductor gamma-spectrometry // *Meas. Tech.* 1993, v. 36, p. 90-93. https://doi.org/10.1007/BF00986185
16. M.I. Romanyuk, J.J. Hainysh, Y. Plakosh, et al. Microtron M-30 for radiation experiments: formation and control of irradiation fields // *Problems of Atomic Science and Technology*. 2022, N 3(1390, p. 137-143. doi:10.46813/2022-139-137
17. О.О. Парлаг, В.Т. Маслюк, А.М. Довбня та інш. *Застосування карбіду бору B_4C для очищення пучків гальмівного випромінювання електронних прискорювачів*: Патент на корисну модель № 96384 від 10.02.2015. (Бюлетень № 2 від 10.02.2015 р.) (in Ukrainian).
18. GEANT4 10.7 (4 December 2020). https://geant4.web.cern.ch/support/download
19. Evaluated Nuclear Data File (ENDF). Database Version of 2022-04-22. https://www-nds.iaea.org/exfor/endf.htm
20. J.D.T. Arruda Neto, S.B. Herdade, B.S. Bhandari, I.C. Nascimento. Electrofission and photofission of ^{238}U in the energy range 6…60 MeV // *Phys. Rev. C*. 1976, v. 14, p. 1499-1505. https://doi.org/10.1103/PhysRevC.14.1499
21. U. Kneissl, H. Ströher, R.D. Fischer, et al. Investigation of the fission decay of the GQR in ^{238}U by e^-- and e^+-induced fission, and tests of DWBA virtual photon spectra / David, P., Mayer-Kuckuk, T., van der Woude, A. (eds). *Dynamics of Nuclear Fission and Related Collective Phenomena.* Lecture Notes in Physics, 1982, v. 158, p. 268-276. https://doi.org/10.1007/BFb0021526
22. I.V. Pylypchynets, O.O. Parlag, E.V. Oleynikov. Simulation the yields of actinide nuclei photofission products induced by bremsstrahlung of electron accelerators // *Scientific Herald of Uzhhorod University. Series "Physics"*. 2017, v. 42, p. 169-177. https://doi.org/10.24144/2415-8038.2017.42.169-177
23. TALYS-1.96. Release date: December 30, 2021. https://tendl.web.psi.ch/tendl_2021/talys.html
24. TENDL-2021 Nuclear data library. Last update: February 23, 2022. Available from: https://tendl.web.psi.ch/tendl_2021/tendl2021.html
25. GEF 2023/1.1. Release: January 12, 2023. http://www.khschmidts-nuclear-web.eu/GEF-2023-1-1.html
26. A.I. Lengyel, O.O. Parlag, V.T. Maslyuk. Semiempirical description of Ge(Li)- and HPGe-detectors efficiency for potofission experiments // *Scientific Herald of Uzhhorod University. Series "Physics"*. 2009, v. 25, p. 95-99.
27. I. Pylypchynets, A. Lengyel, O. Parlag, et al. Empirical formula for the HPGe-detector efficiency dependence on energy and distance // *J. Rad. Nucl. Chem.* 2019, v. 319, p. 1315-1319. https://doi.org/10.1007/s10967-019-06426-8
28. О.О. Парлаг, В.Т. Маслюк, А.М. Довбня, та інш. *Спосіб виготовлення мультинуклідного джерела гамма-випромінювання для калібрування напівпровідникових детекторів за абсолютною ефективністю*: Патент України на корисну модель №130235 (Бюлетень №22 від 26.11.2018 р.).
29. Decay Radiation database version of 3/25/2022, https://www.nndc.bnl.gov/nudat2/indx_dec.jsp
30. M.V. Strilchuk. User manual for Winspectrum. KINR NAS of Ukraine (unpublished). Private communication.
31. C. Agarwal, A. Goswami, P. C. Kalsi, et al. Mass yields in ^{229}Th(n,f) // *J. Radioanal Nucl. Chem.* 2008, v. 275, p. 445-451. https://doi.org/10.1007/s10967-007-7011-8
32. F. James, M. Ross. Function minimization and error analysis. MINUIT D506. CEREN Computer Centre Program library, 1967, p. 1-47.

Article received 13.03.2023

СТРУКТУРА МАСОВИХ РОЗПОДІЛІВ ВИХОДІВ ПРОДУКТІВ ФОТОПОДІЛУ ^{238}U ПРИ ЕНЕРГІЇ ГАЛЬМІВНИХ ФОТОНІВ 17,5 МеВ

Є.В. Олейніков, О.О. Парлаг, І.В. Пилипчинець, В.Т. Маслюк, О.І. Лендел

Значення 29-ти відносних виходів продуктів, що належать 26-ти масовим ланцюжкам фотоподілу ^{238}U, були отримані при максимальній енергії гальмівного випромінювання 17,5 МеВ (біля порога другого шансу поділу). Стимуляція реакції фотоподілу ^{238}U проводилася на електронному прискорювачі Інституту електронної фізики НАН України – мікротроні М-30. Для моделювання компонент спектра гальмівного випромінювання використовувався інструментарій GEANT4. Встановлено наявність тонкої структури в масовому розподілі виходів важких продуктів, яка локалізована в області мас 133-134, 138-139 і 143-144. Для теоретичного описання структури використано мультигаусову модель (суперпозицію трьох гаусіанів). Розраховані значення виходів продуктів з використанням GEF-коду у загальних рисах описують і прогнозують тонку структуру масового розподілу продуктів фотоподілу ^{238}U.